

Ultrafast nanoscale magnetic switching via intense picosecond electron bunches

A. F. Schäffer^{1,*}, H. A. Dürr², J. Berakdar¹

¹*Institut für Physik, Martin-Luther-Universität Halle-Wittenberg,
06099 Halle (Saale), Germany and*

²*Stanford Institute for Materials and Energy Sciences,
SLAC National Accelerator Laboratory,
2575 Sand Hill Road, Menlo Park, California 94025, USA*

(Dated: July 28, 2017)

arXiv:1707.08838v1 [cond-mat.mes-hall] 27 Jul 2017

Abstract

The magnetic field associated with a picosecond intense electron pulse is shown to switch locally the magnetization of extended films and nanostructures and to ignite locally spin waves excitations. Also topologically protected magnetic textures such as skyrmions can be imprinted swiftly in a sample with a residual Dzyaloshinskii-Moriya spin-orbital coupling. Characteristics of the created excitations such as the topological charge or the width of the magnon spectrum can be steered via the duration and the strength of the electron pulses. The study points to a possible way for a spatiotemporally controlled generation of magnetic and skyrmionic excitations.

I. INTRODUCTION

Ultrafast electron microscopy, the introduction of temporal resolution to conventional 3-dimensional electron microscopy, has opened up the space-time exploration of as diverse as nanomaterials and biostructures [1]. Novel electron optical concepts promise a tremendous increase in temporal and spatial resolution allowing researchers to address new scientific challenges [2–6]. The use of relativistic MeV electron energies is an attractive avenue to deal with the issue of Coulomb repulsion in ultrashort electron pulses bringing single-shot electron microscopy on nm length- and ps time-scales within reach [7, 8]. Electrons with MeV energy travel close to the speed of light. This reduces dramatically the velocity mismatch between the electromagnetic pump and electron probe pulses in time-resolved diffraction experiments [9]. This has proven indispensable in probing ultrafast processes in fields ranging from gas-phase photochemistry [10] over lattice transformation in low-dimensional systems [11] to the excitation of transient phonons [12].

While the use of electron pulses as structural dynamics probes is well established, their use as initiators of dynamical processes has remained almost completely unexplored. In an early study, Tudosa *et. al* used the electromagnetic fields surrounding intense relativistic electron pulses to permanently switch the magnetization direction of ferromagnetic films used in magnetic data storage applications [13]. Here we show that nanofocused relativistic electron pulses provide a unique tool to drive and control magnetization dynamics in nanostructures relevant for spintronics applications [13, 14]. The paper is organized as follows. After this introduction, we will describe how our model calculations are able to reproduce the experimental results of Tudosa *et. al* [13]. We will then show how nanofocused electron

beams are able to induce switching and magnon excitations in nanowires and can alter the chirality of skyrmions in nanodots. The paper finishes with conclusions and a brief outlook to possible experimental realizations.

Very recently we published a related work, which deals not only with nanostructured materials but also with extended thin films, possessing Dzyaloshinskii-Moriya interaction (DMI)[15]. There, the creation of skyrmions aside from geometrical confinement is discussed based on the same methods like in this manuscript and is recommended for further reading.

II. RESULTS AND DISCUSSION

A. Electron beam induced magnetic switching

1. Methods

For the purpose of investigating the dynamics of thin magnetic films, micromagnetic simulations solving the Landau-Lifshitz-Gilbert equation (LLG)[16, 17] are executed. The different magnetic systems are discretized into cuboid lattices, so that each simulation cell is associated with a magnetization $\mathbf{m}_i = \mathbf{M}_i/M_S$ normalized to the saturation magnetization M_S . The magnetization dynamics is governed by the LLG

$$\dot{\mathbf{m}}_i = -\frac{\gamma}{1 + \alpha^2} \left\{ \mathbf{m}_i \times \mathbf{H}_i^{\text{eff}}(t) + \alpha \left[\mathbf{m}_i \times (\mathbf{m}_i \times \mathbf{H}_i^{\text{eff}}(t)) \right] \right\} . \quad (1)$$

Here $\gamma = 1.76 \cdot 10^{11} \text{ 1/(Ts)}$ denotes the gyromagnetic ratio and α is the dimensionless Gilbert damping parameter. The local effective magnetic field $\mathbf{H}_i^{\text{eff}}(t)$ can be calculated following the equation $\mu_0 \mathbf{H}_i^{\text{eff}}(t) = -1/M_S \delta F / (\delta \mathbf{m}_i)$ and is therefore a functional of the system's total free energy $F = F_{\text{EXCH}} + F_{\text{MCA}} + F_{\text{DMF}} + F_{\text{ZMN}} + F_{\text{DMI}}$. This quantity is influenced by the exchange interaction of adjacent magnetic moments $F_{\text{EXCH}} = -A/c^2 \sum_{\langle ij \rangle} \mathbf{m}_i \cdot \mathbf{m}_j$, the magnetocrystalline anisotropy F_{MCA} , the demagnetizing fields F_{DMF} , the Zeeman-energy F_{ZMN} and the DMI term F_{DMI} . Further details on the single contributions can be found for example in ref.[18, 19]. In order to simulate the magnetization dynamics an adaptive Heun solver method has been used. As the excitations of the systems take place in a very short time scale the time step is fixed to 1 fs during the time evolution. Using the simulation package `mumax3`[19] full GPU-based micromagnetic calculations are employed to account for the effect of demagnetizing fields efficiently.

As the external magnetic fields, generated by short electron pulses are the main driving mechanism via the Zeeman-coupling, the calculation of these Oersted-like fields is required. The near-field of the electron bunch becomes important for the nanostructures treated in sections II B and II C. We assume a pulse of electrons with a Gaussian envelope in space and in time or accordingly the propagation direction $j_z(r, \varphi, z) = \frac{N_e e v}{(2\pi)^{3/2} \sigma_{xy}^2 \sigma_z} \exp \left[-\frac{1}{2} (r/\sigma_{xy})^2 - \frac{1}{2} ((z - tv)/\sigma_z)^2 \right]$. The parameter N_e corresponds to the number of electrons, e is the electron charge, v the average velocity and σ_{xy} and σ_z are the standard deviations in the related directions. The field's profile resulting from Biot-Savart's law $\mathbf{B}(\mathbf{r}) = \frac{\mu_0}{4\pi} \int_V \mathbf{j}(\mathbf{r}') \times \frac{\mathbf{r} - \mathbf{r}'}{|\mathbf{r} - \mathbf{r}'|^3} dV'$, is shown in fig. 1 for two different sets of parameters. Because of the electron packet propagating in z -direction, the magnetic field consists of the B_φ -component only as inferred from Biot-Savart's law in cylindrical coordinates. The curves shapes are almost the same, as in both cases the radial extension of the beam is much smaller than the standard deviation in the propagation direction. If this is changed the profiles do change as well. The peak field strength for the $30 \mu\text{m}$ beam is ten times smaller than the other pulse. This can be deduced from the number of electrons being a hundred times larger, but contrary the beam width is a thousand times wider, which leads to a resulting factor of 10. For subsequent calculations, the numerical results for the magnetic field are fitted with a model function, which is dependent on both the beam's standard deviation and the included number of electrons, which are experimentally well accessible parameters.

2. Verification of the model

In the past years, multiple experiments exploring the field of magnetic switching triggered by fast electrons have been established. One pioneering example can be found in ref.[13]. In this experiment, short electron bunches are shot through thin films (thickness $\approx 14 \text{ nm}$) of granular CoCrPt-type, in order to explore the ultimate speed limit for precessional magnetic dynamics. The electron pulses have a duration of $\sigma_t = 2.3 \text{ ps}$ a spatial extent of $\sigma_{xy} = 30 \mu\text{m}$ and included a number of $N_e = 10^{10}$ electrons each. After the irradiation, the magnetic domain structure is analyzed, which reveals several domain-wall rings with out-of-plane orientation (fig. 2(a)). Starting from a homogeneously magnetized state in $\pm z$ direction the magnetic moments precess around the \hat{e}_ρ unit vector during the pulse and relax either up

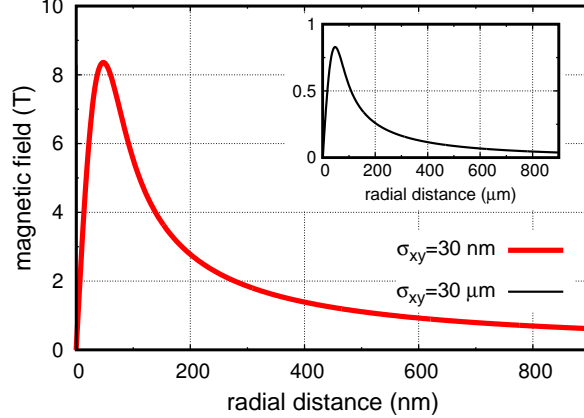


FIG. 1: Radial dependence of the peak magnetic field for a pulse duration of $\sigma_t = 2.3$ ps. The red curve corresponds to $\sigma_{xy} = 30$ nm and $N_e = 10^8$, whereas the black line relates to $\sigma_{xy} = 30$ μm and $N_e = 10^{10}$.

or down afterward. Most of the materials used for magnetic data storage media possesses uniaxial magnetocrystalline anisotropy. CoCrPt-alloys are no exclusion, with an easy axis in the out-of-plane direction, which coincides with the cylindrical z -axis. The material specific parameters are chosen to be equal to the measured ones [13], meaning a saturation magnetization $M_{\text{sat}} = 517.25$ kA/m, the uniaxial anisotropy $K_u = 156.98$ kJ/m³ and the Gilbert damping parameter $\alpha = 0.3$. Similar to the experimental work, we also consider a thin film of CoCrPt and a size of $150 \mu\text{m} \times 150 \mu\text{m} \times 14$ nm. As the included Co-atoms lead to a granular structure, with decoupled magnetic grains with a size of 20.6 ± 4 nm, we can model the system with discrete cells with a dimension of $(41.2 \times 41.2 \times 14)$ nm³. To cover the desired area we need 3640^2 cells. Subsequent to the time propagation over $300\sigma_t$, the magnetic configuration is relaxed, which means that the precessional term in the LLG is disregarded in order to achieve a fast approach towards the final stable magnetic configuration.

The pulse induced ring pattern of the magnetic domains pointing either up or down (with respect to the easy direction of the magnetic films) is well captured by our micromagnetic simulations. As pointed out in [13], the critical precessional angle $\phi \geq \pi/2$ is determined by the local strength of the magnetic field and indicates the achieved angular velocity ω . The pulse duration σ_t plays a crucial role [20–22]. As discussed in Ref.[20–22], an appropriate sequence of ps pulses allows for an optimal control scheme achieving a ballistic magnetic

switching, even in the presence of high thermal fluctuations. Longer pulses might drive the system back to the initial state [20–22]. So, the critical precessional angle and σ_t are the two key parameters [13] for the established final precessional angle $\phi = \omega\sigma_t$. Note, the demagnetization fields are also relevant, as inferred from Fig. 2 but they do not change the main picture.

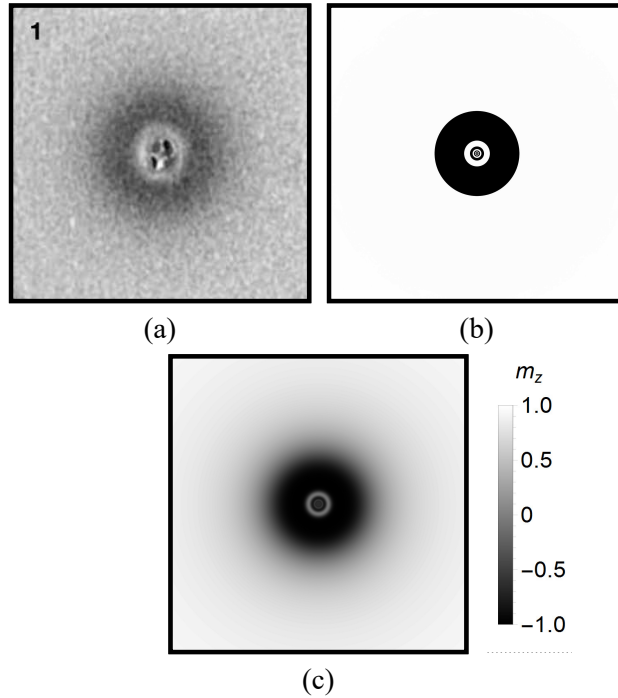


FIG. 2: Comparison between experimental (a)[13], and numerical results (b), (c). Both numerical simulations and the experimental data cover an area of $150 \times 150 \mu\text{m}^2$. In contrast to the panel (b), in (c) the demagnetizing fields are included in simulations. The gray shading signals the magnetization’s z -component with white color meaning $m_z = +\hat{e}_z$ and black $m_z = -\hat{e}_z$. The $N_e = 10^{10}$ electrons in the beam impinging normal to the sample have an energy of 28 GeV. The pulse’s time-envelope is taken as a Gaussian with a pulse duration of $\sigma_t = 2.3$ ps, whereas $\sigma_{xy} = 30 \mu\text{m}$. The generated Oersted field has an equivalent time-dependence.

B. Nanoscale magnetization dynamics

Having substantiated our methods against experiment we turn to the main focus of our study, to be specific the generation of magnetic excitations on the nanoscale. One possible application can be found regarding nanowire geometries. Our aim is to excite such magnetic systems in two different ways. Obviously, the creation of domain walls analogously to the CoCrPt-system discussed before should be possible. On top of this, the confined system leads to a unidirectional transport of spin-waves, also called magnons, which are stimulated by the abrupt excitation of the magnetic moments close to the beam. This setup becomes interesting for strongly focused beams, that cause magnon-modes beyond the linear-response regime, as the LLG couples the magnetization to the demagnetizing fields, which again act on the magnetization dynamics.

We choose a nanowire with a size of $4000 \times 50 \times 2 \text{ nm}^3$, which corresponds to a system of $2000 \times 25 \times 1$ simulation cells. The material parameters are the same as the ones before adapted from the experiment, except for the Gilbert damping parameter, which is reduced to $\alpha = 0.001$ in order to incorporate magnonic excitations. In practice, this can be achieved by preventing the system from exhibiting granular structures. Even if the reduction is not sufficient for this material, the principle can be transferred easily to other thin magnetic films with out-of-plane anisotropy. The electron beam's duration is $\sigma_t = 2.3$ as before, whereas the number of electrons is reduced, but focused on the nanoscale and striking at nanowire's center.

Two different examples are shown in fig. 3 and fig. 4. The graphics show the magnetization's components' time propagation, averaged over the wire's breadth. In fig. 3 a number of $N_e = 5 \times 10^6$ electrons is bundled on a normal distribution with $\sigma_{xy} = 100 \text{ nm}$. A few things in the magnetization are worth to be mentioned. Most distinctly is the creation of two regions with inverted magnetization near the beam's center ($50 \text{ nm} \leq |x| \leq 300 \text{ nm}$). The outer border regions show a Néel type domain wall, whereas the region in between the two domains features a rotating behavior of the in-plane components, which will relax towards a single- or two-domain state on a longer time-scale. On top of this two branches of magnons, propagating along the wire are present. One rather fast propagating spin-wave of minor amplitude and one more pronounced magnon possessing a smaller group velocity. By increasing the beam's intensity ($\sigma_{xy} = 100 \text{ nm}$, $N_e = 5 \times 10^7$) the resulting magneti-

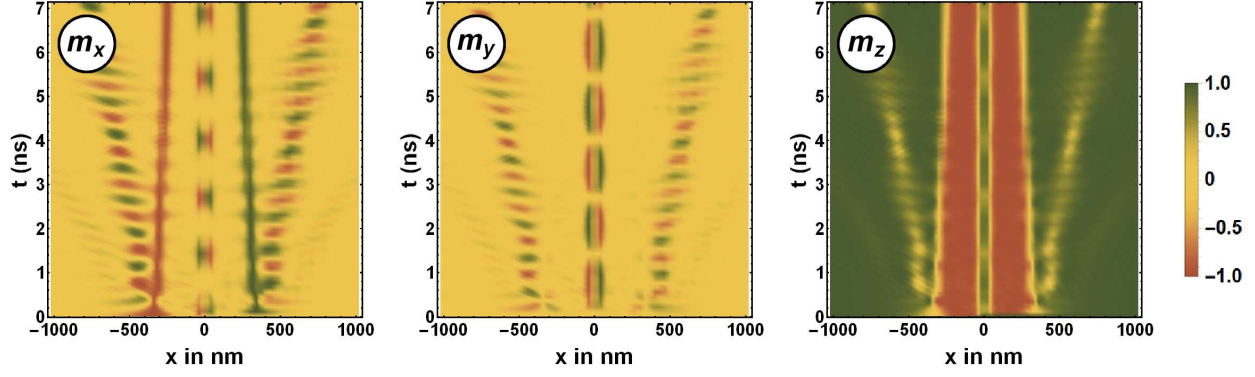


FIG. 3: Time propagation of the magnetization's components for a nanowire of $4000 \times 50 \times 2 \text{ nm}^3$ size and electron beam parameters being $\sigma_t = 2.3$, $\sigma_{xy} = 100 \text{ nm}$ and $N_e = 5 \times 10^6$.

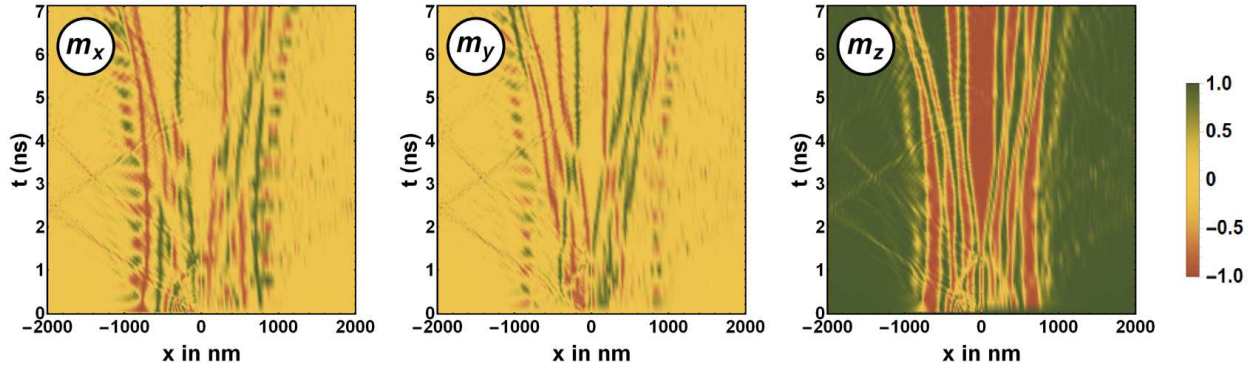


FIG. 4: Time propagation of the magnetization's components for a nanowire of $4000 \times 50 \times 2 \text{ nm}^3$ size and electron beam parameters being $\sigma_t = 2.3$, $\sigma_{xy} = 30 \text{ nm}$ and $N_e = 5 \times 10^7$.

zation dynamics become more complex and multiple branches of magnons interfering with each other, but also domain-walls propagating along the wire can be observed (see fig. 4). Especially rapidly moving magnons, which are reflected by the simulation boxes boundaries are present. Because of the magnetization's non-linear feedback in terms of the demagnetizing fields, a complex pattern occurs. This can be used to analyze magnon-excitation in nanostructures beyond linear-response.

C. Imprinting of topological magnetic structures

The generation of topologically protected magnetic excitations such as skyrmions via pulsed electron pulses is another possible application for the established method. A recent work [23] evidences that ultra thin nanodiscs of materials such $\text{Co}_{70.5}\text{Fe}_{4.5}\text{Si}_{15}\text{B}_{10}$ [24] sandwiched between Pt and Ru/Ta are well suited for our purpose since they exhibit Dzyaloshinskii-Moriya (DM) spin-orbital coupling. Hence the magnetization's structure may nucleate spontaneously into skyrmionic configurations. We adapted the experimentally verified parameters for this sample and present results for the magnetic dynamics triggered by short electron beam pulses.

Taking a nanodisc of a variable size the ground state with a topological number $|N| = 1$ is realized after propagating an initially homogeneous magnetization in $\pm z$ direction according to the Landau-Lifshitz-Gilbert equation (LLG) including DM interactions [16–19]. The two possible ground states, depending on the initial magnetization's direction are shown in fig. 5 along with the material's parameters.

Our main focus is on how to efficiently and swiftly switch between these skyrmion states via a nano-focused relativistic electron pulse, an issue of relevance when it comes to fundamental research or practical applications like data storage. While currently such pulses can be generated with micron size beam dimensions [9] future sources are expected to reach focus sizes down to the few nm range [6]. In principle the possibility of beam damage occurring in the beams focus as in the case of the experiment in ref.[13] is present. However, ongoing experiments with relativistic electron beams [9] indicate that the use of ultrathin freestanding films may alleviate damage concerns.

Topologically protected magnetic configurations, like magnetic skyrmions, are well defined quasiparticles. They can be characterized mathematically by the topological number $N = \frac{1}{4\pi} \int \mathbf{m} \cdot \left(\frac{\partial \mathbf{m}}{\partial x} \times \frac{\partial \mathbf{m}}{\partial y} \right) dx dy$ [25] also called winding number, which counts how often the unit vector of the magnetization wraps the unit sphere when integrated over the two-dimensional sample. Therefore, skyrmions are typically a quasiparticle in thin (mono)layers. The topological number adopts integer values indicating the magnetic configuration to be skyrmionic ($N = \pm 1$) or skyrmion multiplexes ($|N| > 1$). If the topological number is not an integer the topological protection is lifted and the magnetic texture is unstable upon small perturbations. The topological stability of skyrmionic states stem from the necessity

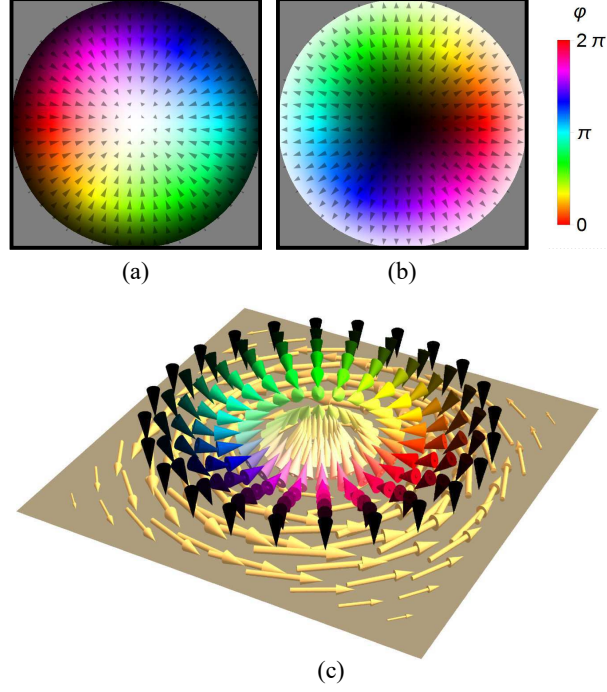


FIG. 5: Magnetic ground states for a nanodisc with a diameter of 300 nm and a thickness of 1.5 nm. The material parameters are $M_{\text{sat}} = 450 \times 10^3 \text{ A/m}$, $A_{\text{ex}} = 10 \text{ pJ/m}$, $\alpha = 0.01$, $K_u = 1.2 \times 10^5 \text{ J/m}^3$ (out-of-plane anisotropy), and the interfacial DMI-constant $D_{\text{ind}} = 0.31 \times 10^{-3} \text{ mJ/m}^2$. (a) corresponds to $N = 1$, whereas (b) possesses $N = -1$, both skyrmions are of the Néel type. Bottom panel illustrates pictorially the influence of the magnetic field associated with the electron bunch. The cones correspond to the initial magnetic configuration as in (a) and (b), whereas the golden arrows show the induced magnetic field. The resulting torque points perpendicular to the magnetization, affecting the magnetic configuration accordingly.

of flipping at least one single magnetic moment by 180° , to overcome the barrier and transfer the state into a "trivial" state, like a single domain or vortex texture. In the following, we will attempt to overcome this topological energy barrier with a magnetic "kick" so that the magnetization will be converted into a state of different topological invariant. Advantageous is the spatial structure of the magnetic field curling around the beam's center, which gives a good point of action in order to manipulate topologically protected configurations.

For magnetic systems, a minimum time of exposure is necessary, whereas the spatial focus of the beam is limited. To overcome this conflict, the pulse duration is fixed at 2.3 ps as

before, when nothing different is mentioned. Starting from such an electron beam two main parameters can be adjusted to achieve the favored reaction of the nanodiscs. Those are the pulse width and the number of electrons, which will be treated independently. In fig. 6, the final topological charges after a single Gaussian electron pulse irradiating a nanodisc are plotted as a function of the number of electrons and the width of the Gaussian distributed electrons. The results do not show the transient time evolution of the sample but only the final steady-state values of the winding number. They are obtained by applying an electron pulse, propagating the magnetization during the pulse, and relaxing the magnetic configuration afterward as to approach a local minimum of the free energy's hypersurface. We note the strong correlation between the change of the topological charge and the number of electrons or accordingly the beam width. Relatively large intervals of both parameters lead to the same final values for N . We note that not only the variation of these control parameters, but also of the duration of the pulse is experimentally accessible, particularly in a nano-apex ultrafast transmission electron microscope [26–43]. Noteworthy, the graphs for opposite initial configurations (see fig. 6(a)) are axially symmetric with respect to the x axis. This can be explained by the coinciding symmetry centers of the pulse and the skyrmionic structure. This symmetric and robust behavior can be exploited to switch between the accessible different values for the topological charges which are quite close to the ideal integer values that would be realized in an infinitely small discretization.

Interestingly, the switching between the two stable states occurs repetitively for an increase in the number of electrons, whereas the spatial manipulation of the beam leads to one regime only in which the fields are sufficient to switch the topological number. The first observation can be explained with the schematics shown in fig.5c). Depending on the strength of the pulse the magnetic moments are forced to rotate multiple times around the \hat{e}_φ vector in a collective manner, as each moment of equal distance to the center experiences the same torque. The final position of the surrounding moments couples backward to the center and determines the new topological charge. The electron number linearly translates to the peak magnetic field, whereas the beam width has a more complicated influence. When the width is increased the spatial profile in the xy -plane is manipulated, as the maximum magnetic field is shifted towards the disc's rim and beyond. How the system reacts on this changes depends crucially on the exact profile of the beam, especially on the point of maximum magnetic field strength, as can be seen in fig. 6(a). This leads to the question of the optimum

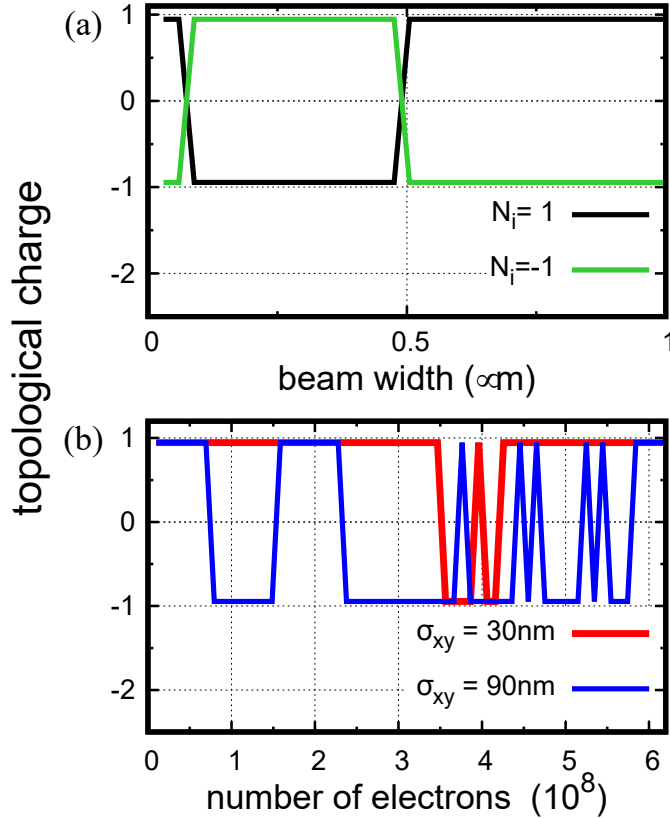


FIG. 6: Varying the number of electrons per pulse or the spatial enlargement of the pulse, the imprinted topological charge can be tuned. The pulse duration is set to 2.3 ps. Black and green curves correspond respectively to starting with a magnetic ordering having +1 or -1 topological charge, as shown in fig. 5 for different pulse widths. Both the blue and red curve start from $N_i = +1$. The sample is a magnetic disc (diameter $d = 300$ nm) which is irradiated with a Gaussian beam pulse with $\sigma_{xy} = 30$ nm (and 90 nm) in case of the bottom graph, respectively the upper graphs' beam has a constant number of $n_e = 10^8$ electrons.

parameter regime, to manipulate the system reliably, which can not finally be answered as it strongly depends on the experimentally available capabilities. Hence this work focuses on an exemplary study on the effect.

The same switching phenomenon as discussed before can also be observed for different setups. Weaker pulses, as long as they are able to overcome the internal fields to excite the system, can be used as well, but obviously, the field's amplitude translates to the strength of the resulting torque. This implies a longer radiation time needed for pulses of lower intensity to be capable of switching the system.

In the case of different materials or geometries, the accessible topological states have to be investigated, before they can be utilized. Otherwise undesired, interstitial states might be achieved by accident and the switching is not deterministic anymore.

III. SUMMARY AND OUTLOOK

We have shown using micromagnetic calculations that relativistic electron pulses of few ps duration can indeed induce magnetization dynamics in ferromagnetic nanostructures and extended films as observed experimentally [13]. Contrary to micron sized electron beams employed experimentally so far [13], nanofocusing allows us to reduce the number of electrons dramatically in order to achieve magnetic switching. We demonstrated this for the case of ferromagnetic nanowires where the nanofocused electron pulses enabled magnetic switching on one end of the wire with magnon excitations propagating along the wire towards the other end. We also predict a novel way of switching the winding sense of magnetic skyrmions using the tangential fields of electron pulses focused down to the skyrmion size. We predict that such magnon excitations can be driven with electron numbers as low as 10^6 electrons/pulse. This is within reach at present electron diffraction experiments [9]. Attempts at achieving the required nanofocus at such sources are currently underway. We note that the predicted magnetization dynamics could be imaged using VUV [44] and soft x-ray photons [45]. Since both ultrafast electron diffraction and imaging experiments start with laser-generated photoelectrons the synchronization of fs probe laser systems with the electron pulses is straightforward [9]. The necessary probing of magnetization dynamics has recently been demonstrated using circularly polarized photons for high-harmonic laser sources [46].

ACKNOWLEDGMENTS

A. F. S. and J. B. are supported by the German Research Foundation (No. SFB 762) and the Priority Programme 1840. H.A.D. acknowledges support by the U.S. Department of Energy, Office of Basic Energy Sciences, Materials Sciences and Engineering Division under

- [1] Ahmed H Zewail. Four-dimensional electron microscopy. *Science*, 328(5975):187–193, 2010.
- [2] Alexander Paarmann, M Gulde, Melanie Müller, S Schäfer, S Schweda, M Maiti, C Xu, T Hohage, F Schenk, C Ropers, et al. Coherent femtosecond low-energy single-electron pulses for time-resolved diffraction and imaging: A numerical study. *Journal of Applied Physics*, 112(11):113109, 2012.
- [3] Johannes Hoffrogge, Jan Paul Stein, Michael Krüger, Michael Förster, Jakob Hammer, Dominik Ehberger, Peter Baum, and Peter Hommelhoff. Tip-based source of femtosecond electron pulses at 30 keV. *Journal of Applied Physics*, 115(9):094506, 2014.
- [4] Armin Feist, Katharina E Echternkamp, Jakob Schauss, Sergey V Yalunin, Sascha Schäfer, and Claus Ropers. Quantum coherent optical phase modulation in an ultrafast transmission electron microscope. *Nature*, 521(7551):200–203, 2015.
- [5] Max Gulde, Simon Schweda, Gero Storeck, Manisankar Maiti, Hak Ki Yu, Alec M Wodtke, Sascha Schäfer, and Claus Ropers. Ultrafast low-energy electron diffraction in transmission resolves polymer/graphene superstructure dynamics. *Science*, 345(6193):200–204, 2014.
- [6] Yimei Zhu and Hermann Dürr. The future of electron microscopy. *Physics Today*, 68(4):32, 2015. doi:10.1063/PT.3.2747.
- [7] RK Li and P Musumeci. Single-shot mev transmission electron microscopy with picosecond temporal resolution. *Physical Review Applied*, 2(2):024003, 2014.
- [8] D. Xiang, F. Fu, J. Zhang, X. Huang, L. Wang, X. Wang, and W. Wan. Accelerator-based single-shot ultrafast transmission electron microscope with picosecond temporal resolution and nanometer spatial resolution. *Nuclear Instruments and Methods in Physics Research Section A: Accelerators, Spectrometers, Detectors and Associated Equipment*, 759:74 – 82, 2014. ISSN 0168-9002. doi:http://dx.doi.org/10.1016/j.nima.2014.05.068. URL <http://www.sciencedirect.com/science/article/pii/S0168900214006081>.
- [9] SP Weathersby, G Brown, Martin Centurion, TF Chase, Ryan Coffee, Jeff Corbett, JP Eichner, JC Frisch, AR Fry, M Gühr, et al. Mega-electron-volt ultrafast electron diffraction at slac national accelerator laboratory. *Review of Scientific Instruments*, 86(7):073702, 2015.

- [10] Jie Yang, Markus Guehr, Xiaozhe Shen, Renkai Li, Theodore Vecchione, Ryan Coffee, Jeff Corbett, Alan Fry, Nick Hartmann, Carsten Hast, et al. Diffractive imaging of coherent nuclear motion in isolated molecules. *Physical review letters*, 117(15):153002, 2016.
- [11] Ehren M Mannebach, Renkai Li, Karel-Alexander Duerloo, Clara Nyby, Peter Zalden, Theodore Vecchione, Friederike Ernst, Alexander Hume Reid, Tyler Chase, Xiaozhe Shen, et al. Dynamic structural response and deformations of monolayer mos2 visualized by femtosecond electron diffraction. *Nano letters*, 15(10):6889–6895, 2015.
- [12] T Chase, M Trigo, AH Reid, R Li, T Vecchione, X Shen, S Weathersby, R Coffee, N Hartmann, DA Reis, et al. Ultrafast electron diffraction from non-equilibrium phonons in femtosecond laser heated au films. *Applied Physics Letters*, 108(4):041909, 2016.
- [13] I Tudosa, Ch Stamm, AB Kashuba, F King, HC Siegmann, J Stöhr, G Ju, B Lu, and D Weller. The ultimate speed of magnetic switching in granular recording media. *Nature*, 428(6985):831–833, 2004.
- [14] Benjamin Lenk, Henning Ulrichs, Fabian Garbs, and Markus Münzenberg. The building blocks of magnonics. *Physics Reports*, 507(4):107–136, 2011.
- [15] Alexander F Schäffer, Hermann A Dürr, and Jamal Berakdar. Ultrafast imprinting of topologically protected magnetic textures via pulsed electrons. *Applied Physics Letters*, page to appear, 2017.
- [16] LALE Landau and Evgeny Lifshitz. On the theory of the dispersion of magnetic permeability in ferromagnetic bodies. *Phys. Z. Sowjetunion*, 8(153):101–114, 1935.
- [17] TL Gilbert. A lagrangian formulation of the gyromagnetic equation of the magnetization field. *Phys. Rev.*, 100:1243, 1955.
- [18] Alexander Sukhov, Paul P Horley, Jamal Berakdar, Alexandra Terwey, Ralf Meckenstock, and Michael Farle. Dipole–dipole interaction in arrays of fe/fe x o y core/shell nanocubes probed by ferromagnetic resonance. *IEEE Transactions on Magnetics*, 50(12):1–9, 2014.
- [19] Arne Vansteenkiste, Jonathan Leliaert, Mykola Dvornik, Mathias Helsen, Felipe Garcia-Sanchez, and Bartel Van Waeyenberge. The design and verification of mumax3. *Aip Advances*, 4(10):107133, 2014.
- [20] Alexander Sukhov and Jamal Berakdar. Local control of ultrafast dynamics of magnetic nanoparticles. *Physical review letters*, 102(5):057204, 2009.

- [21] A Sukhov and J Berakdar. Steering magnetization dynamics of nanoparticles with ultrashort pulses. *Physical Review B*, 79(13):134433, 2009.
- [22] A Sukhov and J Berakdar. Influence of field orientation on the magnetization dynamics of nanoparticles. *Applied Physics A: Materials Science & Processing*, 98(4):837–842, 2010.
- [23] AG Kolesnikov, AS Samardak, ME Steblyi, AV Ognev, LA Chebotkevich, AV Sadovnikov, SA Nikitov, Yong Jin Kim, In Ho Cha, and Young Keun Kim. Spontaneous nucleation and topological stabilization of skyrmions in magnetic nanodisks with the interfacial dzyaloshinskii–moriya interaction. *Journal of Magnetism and Magnetic Materials*, 429:221–226, 2017.
- [24] BS Chun, SD Kim, YS Kim, JY Hwang, SS Kim, JR Rhee, TW Kim, JP Hong, MH Jung, and YK Kim. Effects of co addition on microstructure and magnetic properties of ferromagnetic cofilin alloy films. *Acta Materialia*, 58(8):2836–2842, 2010.
- [25] Naoto Nagaosa and Yoshinori Tokura. Topological properties and dynamics of magnetic skyrmions. *Nature nanotechnology*, 8(12):899–911, 2013.
- [26] C Ropers, DR Solli, CP Schulz, C Lienau, and T Elsaesser. Localized multiphoton emission of femtosecond electron pulses from metal nanotips. *Physical review letters*, 98(4):043907, 2007.
- [27] Brett Barwick, Chris Corder, James Strohaber, Nate Chandler-Smith, Cornelius Uiterwaal, and Herman Batelaan. Laser-induced ultrafast electron emission from a field emission tip. *New Journal of Physics*, 9(5):142, 2007.
- [28] Peter Hommelhoff, Catherine Kealhofer, and Mark A Kasevich. Ultrafast electron pulses from a tungsten tip triggered by low-power femtosecond laser pulses. *Physical review letters*, 97(24):247402, 2006.
- [29] Peter Hommelhoff, Yvan Sortais, Anoush Aghajani-Talesh, and Mark A Kasevich. Field emission tip as a nanometer source of free electron femtosecond pulses. *Physical review letters*, 96(7):077401, 2006.
- [30] Claus Ropers, Thomas Elsaesser, Giulio Cerullo, Margherita Zavelani-Rossi, and Christoph Lienau. Ultrafast optical excitations of metallic nanostructures: from light confinement to a novel electron source. *New Journal of Physics*, 9(10):397, 2007.
- [31] Hirofumi Yanagisawa, Christian Hafner, Patrick Doná, Martin Klöckner, Dominik Leuenberger, Thomas Greber, Matthias Hengsberger, and Jürg Osterwalder. Optical control of field-emission sites by femtosecond laser pulses. *Physical review letters*, 103(25):257603, 2009.

- [32] Hirofumi Yanagisawa, Christian Hafner, Patrick Doná, Martin Klöckner, Dominik Leuenberger, Thomas Greber, Jürg Osterwalder, and Matthias Hengsberger. Laser-induced field emission from a tungsten tip: Optical control of emission sites and the emission process. *Physical Review B*, 81(11):115429, 2010.
- [33] Markus Schenk, Michael Krüger, and Peter Hommelhoff. Strong-field above-threshold photoemission from sharp metal tips. *Physical review letters*, 105(25):257601, 2010.
- [34] R Bormann, M Gulde, A Weismann, SV Yalunin, and C Ropers. Tip-enhanced strong-field photoemission. *Physical review letters*, 105(14):147601, 2010.
- [35] Michael Krüger, Markus Schenk, and Peter Hommelhoff. Attosecond control of electrons emitted from a nanoscale metal tip. *Nature*, 475(7354):78–81, 2011.
- [36] Doo Jae Park, Bjoern Piglosiewicz, Slawa Schmidt, Heiko Kollmann, Manfred Mascheck, and Christoph Lienau. Strong field acceleration and steering of ultrafast electron pulses from a sharp metallic nanotip. *Physical review letters*, 109(24):244803, 2012.
- [37] G Herink, DR Solli, M Gulde, and C Ropers. Field-driven photoemission from nanostructures quenches the quiver motion. *Nature*, 483(7388):190–193, 2012.
- [38] L Wimmer, G Herink, DR Solli, SV Yalunin, KE Echternkamp, and C Ropers. Terahertz control of nanotip photoemission. *Nature Physics*, 10(6):432–436, 2014.
- [39] Hirofumi Yanagisawa, Matthias Hengsberger, Dominik Leuenberger, Martin Klöckner, Christian Hafner, Thomas Greber, and Jürg Osterwalder. Energy distribution curves of ultrafast laser-induced field emission and their implications for electron dynamics. *Physical review letters*, 107(8):087601, 2011.
- [40] AR Bainbridge and WA Bryan. Velocity map imaging of femtosecond laser induced photoelectron emission from metal nanotips. *New Journal of Physics*, 16(10):103031, 2014.
- [41] RJ Dwayne Miller. Mapping atomic motions with ultrabright electrons: The chemists’ gedanken experiment enters the lab frame. *Annual review of physical chemistry*, 65:583–604, 2014.
- [42] David J Flannigan and Ahmed H Zewail. 4d electron microscopy: principles and applications. *Accounts of chemical research*, 45(10):1828–1839, 2012.
- [43] Judy S Kim, Thomas LaGrange, Bryan W Reed, Mitra L Taheri, Michael R Armstrong, Wayne E King, Nigel D Browning, and Geoffrey H Campbell. Imaging of transient structures using nanosecond in situ tem. *Science*, 321(5895):1472–1475, 2008.

- [44] C von Korff Schmising, B Pfau, M Schneider, CM Günther, M Giovannella, J Perron, B Vodungbo, L Müller, F Capotondi, E Pedersoli, et al. Imaging ultrafast demagnetization dynamics after a spatially localized optical excitation. *Physical review letters*, 112(21):217203, 2014.
- [45] Tianhan Wang, Diling Zhu, Benny Wu, Catherine Graves, Stefan Schaffert, Torbjörn Rander, Leonard Müller, Boris Vodungbo, Cédric Baumier, David P Bernstein, et al. Femtosecond single-shot imaging of nanoscale ferromagnetic order in co/pd multilayers using resonant x-ray holography. *Physical review letters*, 108(26):267403, 2012.
- [46] Tingting Fan, Patrik Grychtol, Ronny Knut, Carlos Hernández-García, Daniel D Hickstein, Dmitriy Zusin, Christian Gentry, Franklin J Dollar, Christopher A Mancuso, Craig W Hogle, et al. Bright circularly polarized soft x-ray high harmonics for x-ray magnetic circular dichroism. *Proceedings of the National Academy of Sciences*, 112(46):14206–14211, 2015.